

Temperature dependence of dielectric, elastic, and piezoelectric constants of [001]_c poled Mn-doped 0.24Pb(In_{1/2}Nb_{1/2})O₃-0.46Pb(Mg_{1/3}Nb_{2/3})O₃-0.30PbTiO₃ single crystal

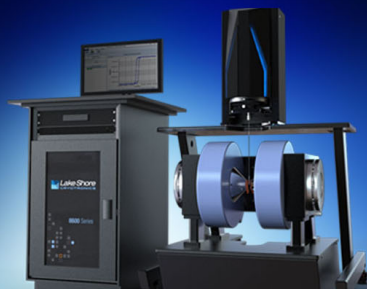
Liguo Tang^{*}, Hua Tian, Yu Zhang, and Wenwu Cao^{*}

Citation: *Appl. Phys. Lett.* **108**, 082901 (2016); doi: 10.1063/1.4942382

View online: <http://dx.doi.org/10.1063/1.4942382>


View Table of Contents: <http://aip.scitation.org/toc/apl/108/8>

Published by the [American Institute of Physics](#)



NEW 8600 Series VSM

For fast, highly sensitive
measurement performance

LEARN MORE 

Temperature dependence of dielectric, elastic, and piezoelectric constants of [001]_c poled Mn-doped 0.24Pb(In_{1/2}Nb_{1/2})O₃-0.46Pb(Mg_{1/3}Nb_{2/3})O₃-0.30PbTiO₃ single crystal

Liguo Tang,^{1,a)} Hua Tian,² Yu Zhang,¹ and Wenwu Cao^{3,b)}

¹Key Laboratory of Underwater Acoustic Communication and Marine information Technology, Ministry of Education, Xiamen University, Xiamen 361005, China

²Institute of Applied Acoustics, Shaanxi Normal University, Xi'an, Shaanxi 710062, China

³Department of Mathematics and Materials Research Institute, The Pennsylvania State University, University Park, Pennsylvania 16802, USA

(Received 24 December 2015; accepted 6 February 2016; published online 22 February 2016)

In order to simulate the performance of electromechanical devices at elevated temperatures, full tensor properties of piezoelectric materials at high temperatures are needed. Such data are extremely difficult to get for relaxor-based single crystals because their properties are determined by domain structures, which are strongly geometry dependent. We report here the temperature dependence of full tensor material constants of [001]_c poled Mn-doped 0.24Pb(In_{1/2}Nb_{1/2})O₃-0.46Pb(Mg_{1/3}Nb_{2/3})O₃-0.30PbTiO₃ single crystals from 25 °C to 55 °C, which were determined by the resonant ultrasound spectroscopy. Because only one sample was used, high degree of self-consistency was achieved for the tensor constants at all measured temperatures. © 2016 AIP Publishing LLC. [<http://dx.doi.org/10.1063/1.4942382>]

The [001]_c poled multidomain relaxor-based single crystals (1-x)Pb(Mg_{1/3}Nb_{2/3})O₃-xPbTiO₃ (PMN-PT) and xPb(In_{1/2}Nb_{1/2})O₃-(1-x-y)Pb(Mg_{1/3}Nb_{2/3})O₃-yPbTiO₃ (PIN-PMN-PT) in the rhombohedral phase possess outstanding piezoelectric and electromechanical properties, and they have already triggered a revolution in ultrasonic imaging transducers, piezoelectric actuators, and sensors in the past two decades.¹⁻³ The ternary PIN-PMN-PT single crystals have higher phase transition temperatures (T_{RT} and T_C) and much larger coercive field E_c, which are advantageous for higher power devices and higher temperature applications.²⁻⁴ It was found that the Q_M of [001]_c poled Mn-doped PIN-PMN-PT single crystals can reach as high as 700–1000, which is comparable to that of hard lead zirconate titanate (PZT) ceramics.^{5,6}

During the operation of high power electromechanical devices, there is often temperature rise due to the mechanical and dielectric losses, causing the degradation of device performance. It is possible to quantify such degradation using finite element simulations, but one must know the full matrix material properties at elevated temperatures. The IEEE impedance resonance technique for measuring the full tensor properties requires at least 5–7 samples of very different geometries, which caused self-consistency problems because the properties of ferroelectric materials depend on poling, while the degree of poling depends on sample geometries.

The temperature dependence of material constants has received a lot of interests because of the need to simulate device performance at elevated temperatures using 3-D finite element methods. There were some published works in the literature on the temperature dependence of material

constants, which revealed the intrinsic physical nature of the material.^{7,8} Sabat *et al.* studied the temperature dependence of the dielectric, elastic, and piezoelectric constants of soft and hard doped PZTs by the IEEE impedance resonant method,⁹ but their results are not self-consistent. Tang and Cao characterized the temperature dependence of the full matrix material constants of PZT-4 ceramics by the resonant ultrasound spectroscopy (RUS) technique, and the obtained full matrix data are highly self-consistent at all measured temperatures.¹⁰ Zhang *et al.* investigated the full matrix constants of Pb(Mg_{1/3}Nb_{2/3})O₃-PbZrO₃-PbTiO₃ single crystals at three different temperatures using several samples with different geometries by the IEEE impedance resonant method, which is insufficient to get the trend of the temperature dependence.¹¹ Generally speaking, the full matrix material constants obtained by the pulse-echo and impedance resonant methods from multiple samples with drastically different geometries may not be self-consistent, and the self-consistency problem becomes worse at higher temperatures. If the tensor data are not self-consistent, quantities calculated using such data would produce unphysical results. For example, the calculated electromechanical coupling factor may exceed 100%, or a calculated quantity using two different formulas will have a large difference.^{12,13}

In this letter, we report the characterization of the temperature dependence of full tensor material constants of a [001]_c poled Mn-doped 0.24PIN-0.46PMN-0.30PT single crystal from 25 °C to 55 °C by using the RUS technique. The RUS technique is to measure the spectrum of mechanical resonances of a sample of nearly a cube. One starts with a set of guessed constants to calculate the spectrum and then adjust them against the measured spectrum using an optimization algorithm. When the calculated and measured spectra match well with each other, the adjusted material constants can be considered the true values of these constants.

^{a)}liguotang@xmu.edu.cn

^{b)}dzk@psu.edu

For the $[001]_c$ poled Mn-doped 0.24PIN-0.46PMN-0.30PT single crystal, the effective macroscopic symmetry is tetragonal $4mm$. There are totally 11 independent material constants: 2 dielectric constants, 3 piezoelectric constants, and 6 elastic constants.

In the RUS measurements, we used a rectangular parallel-epiped sample, whose eigen-modes can be divided into four vibration groups denoted by A_g , B_g , A_u , and B_u according to the symmetries of corresponding displacement patterns.¹⁴ A $[001]_c$ poled 0.5 wt. % Mn-doped 0.24PIN-0.46PMN-0.30PT sample with the dimensions of $4.956 \times 5.416 \times 4.328 \text{ mm}^3$ used for the RUS measurements was cut from a crystal boule grown by a modified Bridgman method (H.C., Materials, USA). The density ρ of the sample is 8117 kg/m^3 . The sample was poled in silicone oil for 30 min at room temperature using an electric field of 15 kV/cm along $[001]_c$. Clamped and free dielectric constants were calculated based on the capacitances measured at 1 kHz and 35 MHz , respectively. The obtained clamped dielectric constants ϵ_{11}^S and ϵ_{33}^S as a function of temperature T can be fitted to the following functions:

$$\epsilon_{11}^S = 6.710 + 1.174 \times 10^{-1}T - 1.245 \times 10^{-3}T^2 + 1.599 \times 10^{-5}T^3 \quad (10^{-9}\text{F/m}), \quad (1)$$

$$\epsilon_{33}^S = 4.716 + 1.270 \times 10^{-2}T + 2.240 \times 10^{-4}T^2 + 5.619 \times 10^{-7}T^3 \quad (10^{-9}\text{F/m}). \quad (2)$$

The DRS Q9000 system connected to a PC was used to measure the vibration resonance spectra at different temperatures, as shown in Fig. 1. The sample, transmitting and receiving transducers were bundled and put into a KSL 1100X oven. The temperature of the sample inside the oven was measured by a Fluke 51 thermometer using a k-type thermocouple. The temperature control of the oven was within 0.1°C .

The resonance spectra were measured from 25°C to 55°C at the temperature step of $\Delta T = 5^\circ\text{C}$. The reason for not going to even higher temperature is because partial domain back-switching occurred at 60°C . Figure 2 shows the resonant ultrasound spectra of the $[001]_c$ poled Mn-doped 0.24PIN-0.46PMN-0.30PT sample from 200 kHz to 400 kHz at 30°C (blue) and 50°C (red), respectively. In order to get sufficient number of modal frequencies, the resonance spectra were measured from 100 kHz to 650 kHz in our case. Experience tells us that the number of resonance frequencies

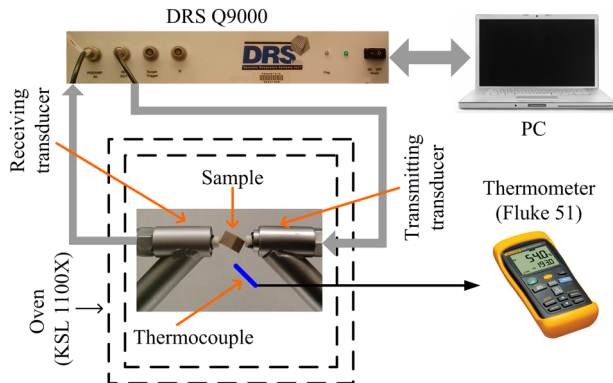


FIG. 1. RUS experimental setup.

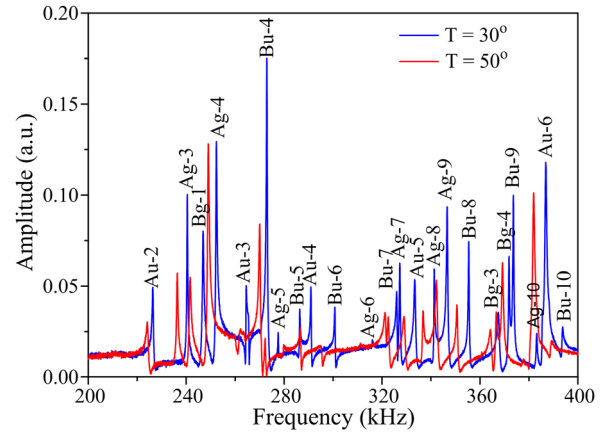


FIG. 2. Resonant ultrasound spectra from 200 kHz to 400 kHz at 30°C (blue) and 50°C (red).

measured and identified should be at least 5 times of the number of independent constants to be determined in order for the RUS technique to function well.¹⁵ During the measurement, the sample was put in between the transmitting and receiving transducers with contacts only at the opposite corners of the sample, as shown in Fig. 1. Therefore, some resonance modes may be missed in the measured spectrum when the receiving corner is the node of certain modes.

It is crucial to correctly identify enough number of modes and accurately determine the material constants at the initial (room) temperature. The mode identification process at the initial temperature can be summarized as follows:

- (1) Determine the clamped dielectric constants ϵ_{11}^S and ϵ_{33}^S , and free dielectric constant ϵ_{11}^T using the HP4294 impedance analyzer;
- (2) Measure the values of c_{11}^E , c_{44}^E , and c_{66}^E using the ultrasonic pulse-echo method;
- (3) Determine the value of e_{15} using the formula $e_{15} = \sqrt{(\epsilon_{11}^T - \epsilon_{11}^S)c_{44}^E}$;
- (4) Measure the resonant ultrasound spectrum from 100 kHz to 650 kHz using the DRS 9000 system;
- (5) Correctly identify at least 25 modes and then use them to determine the values of c_{12}^E , c_{13}^E , c_{33}^E , e_{31} , and e_{33} based on the Levenberg-Marquardt (LM) algorithm.^{16,17}
- (6) Identify more number of modes by using the obtained full matrix material constants to calculate the spectrum and compare it with measured spectrum.

Once the mode corresponding to each measured resonance frequency at the initial temperature is identified, one can follow it to the next temperature step. In our case, 41 modes between 100 kHz and 650 kHz were identified and used in the inversion calculations for higher temperatures.

The process of determining material constants from the measured resonance frequencies is to find a local minimizer of the deviation function

$$F = \sum_{i=1}^K w_i [f_{cal}^{(i)} - f_{meas}^{(i)}]^2, \quad (3)$$

where $f_{meas}^{(i)}$ and $f_{cal}^{(i)}$ are the i th measured and calculated resonance frequencies, respectively, and w_i is the weighting factor.

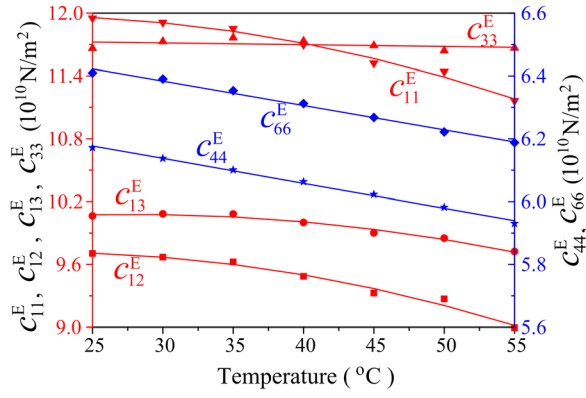


FIG. 3. RUS inversion results of elastic stiffness constants c_{11}^E , c_{12}^E , c_{13}^E , c_{33}^E , c_{44}^E , and c_{66}^E .

In our calculations, the weighting factor w_i is set to $1/f_{meas}^{(i)2}$. MINPACK,¹⁵ which is a well-known FORTRAN library based on LM algorithm, was used in our computational codes.

The data points shown in Figs. 3 and 4 are the inversion results of elastic stiffness constants at constant electric field and piezoelectric stress constants, respectively. The values of full tensor constants at different temperatures are also given in Table I for easy reference. The solid lines in Figs. 3 and 4 are fitted results, which can be described by the following equations:

$$c_{11}^E = 11.73 + 2.483 \times 10^{-2}T - 6.344 \times 10^{-4}T^2 \quad (10^{10}\text{N/m}^2), \quad (4)$$

$$c_{12}^E = 9.440 + 2.606 \times 10^{-2}T - 6.139 \times 10^{-4}T^2 \quad (10^{10}\text{N/m}^2), \quad (5)$$

$$c_{13}^E = 9.697 + 2.738 \times 10^{-2}T - 4.908 \times 10^{-4}T^2 \quad (10^{10}\text{N/m}^2), \quad (6)$$

$$c_{33}^E = 11.76 - 1.685 \times 10^{-3}T \quad (10^{10}\text{N/m}^2), \quad (7)$$

$$c_{44}^E = 6.375 - 7.933 \times 10^{-3}T \quad (10^{10}\text{N/m}^2), \quad (8)$$

$$c_{66}^E = 6.616 - 7.764 \times 10^{-3}T \quad (10^{10}\text{N/m}^2), \quad (9)$$

$$e_{15} = 6.068 + 8.005 \times 10^{-2}T \quad (\text{C/m}^2), \quad (10)$$

$$e_{31} = -(6.477 - 6.848 \times 10^{-2}T + 1.342 \times 10^{-3}T^2) \quad (\text{C/m}^2), \quad (11)$$

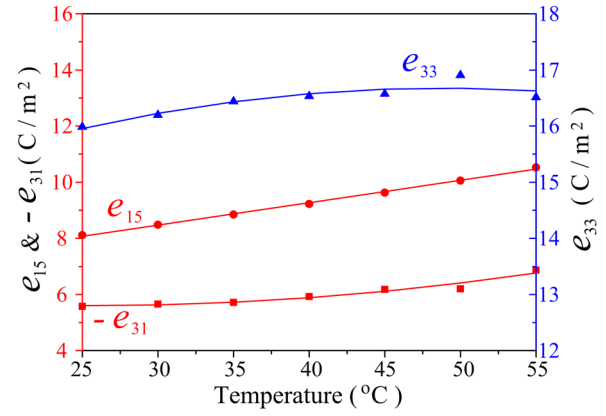


FIG. 4. RUS inversion results of piezoelectric stress constants e_{15} , $-e_{31}$, and e_{33} .

$$e_{33} = 13.64 + 1.244 \times 10^{-1}T - 1.274 \times 10^{-3}T^2 \quad (\text{C/m}^2). \quad (12)$$

Figure 3 shows that the elastic stiffness constants, c_{11}^E , c_{12}^E , c_{13}^E , c_{44}^E , and c_{66}^E , decrease with temperature in the temperature range of 25 °C to 55 °C. Moreover, c_{44}^E and c_{66}^E are nearly linear functions of temperature. The values of c_{11}^E and c_{12}^E decrease by 6.6% and 7.2%, respectively, when the temperature elevates from 25 °C to 55 °C, while c_{33}^E is nearly a constant. The influence of temperature on the elastic constants of [001]_c poled Mn-doped 0.24PIN-0.46PMN-0.30PT single crystals is totally different from that of the elastic constants of lead zirconate titanate (PZT-4) ceramics. The elastic stiffness constants c_{11}^E , c_{33}^E , c_{44}^E of PZT-4 ceramics increase slightly with temperature,¹⁰ but all independent elastic constants except c_{33}^E of [001]_c poled Mn-doped 0.24PIN-0.46PMN-0.30PT single crystals decrease with temperature. Figure 4 shows that the piezoelectric stress constants, e_{15} , $-e_{31}$, and e_{33} , increase with temperature. The values of e_{15} and $-e_{31}$ increased by 29.7% and 23.1%, respectively, when the temperature is increased from 25 °C to 55 °C. The increasing trend of piezoelectric strain constants e_{15} , e_{33} , and $-e_{31}$ is the same as that of PZT-4 ceramics. The stronger temperature dependence of material constants observed in the [001]_c poled Mn-doped 0.24PIN-0.46PMN-0.30PT single crystals is caused by the much lower phase transition temperature compared to that of PZT ceramics.

Comparing our full matrix material constants of [001]_c poled Mn-doped 0.24PIN-0.46PMN-0.30PT single crystals

TABLE I. RUS inversion results of c_{11}^E , c_{12}^E , c_{13}^E , c_{33}^E , c_{44}^E , c_{66}^E , e_{15} , $-e_{31}$, and e_{33} , and the fitted values of e_{11}^S and e_{33}^S from measured results at different temperatures.

T (°C)	RUS inversion results ^a									fitted results	
	c_{11}^E	c_{12}^E	c_{13}^E	c_{33}^E	c_{44}^E	c_{66}^E	e_{15}	e_{31}	e_{33}	$\frac{e_{11}^S}{\epsilon_0}$	$\frac{e_{33}^S}{\epsilon_0}$
25	11.95	9.704	10.06	11.66	6.171	6.409	8.115	-5.576	15.99	1030	585
30	11.91	9.669	10.08	11.72	6.137	6.390	8.481	-5.657	16.20	1078	600
35	11.85	9.623	10.08	11.76	6.101	6.353	8.845	-5.718	16.44	1127	617
40	11.70	9.485	10.00	11.73	6.063	6.312	9.224	-5.926	16.53	1178	635
45	11.52	9.324	9.902	11.69	6.023	6.269	9.626	-6.186	16.58	1234	654
50	11.44	9.269	9.852	11.64	5.982	6.222	10.06	-6.204	16.91	1295	675
55	11.16	8.995	9.723	11.66	5.930	6.188	10.53	-6.871	16.51	1362	699

^aThe unit of elastic constants is 10^{10}N/m^2 , and the unit of piezoelectric constants is C/m^2 .

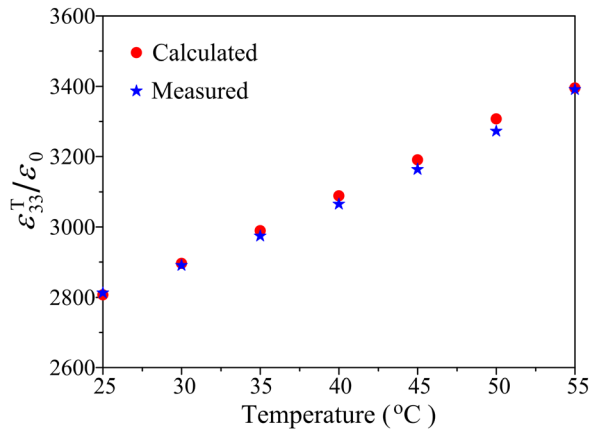


FIG. 5. Comparison between measured and calculated free dielectric constant $\epsilon_{33}^T/\epsilon_0$ in the unit of ϵ_0 .

determined by the RUS technique with those of $[001]_c$ poled Mn-doped 0.24PIN-0.47PMN-0.29PT single crystals by traditional pulse-echo and impedance resonant methods at room temperature,⁵ excellent agreement can be found.

In order to further verify the self-consistency of the obtained complete data set, the measured free dielectric constants ϵ_{33}^T are compared with that of the calculated one by the following equation:

$$\epsilon_{33}^T = \epsilon_{33}^S + 2e_{31}^2(s_{11}^E + s_{12}^E) + 2e_{31}e_{33}s_{13}^E + d_{33}e_{33}, \quad (13)$$

where

$$d_{33} = 2e_{31}s_{13}^E + e_{33}s_{33}^E. \quad (14)$$

Here s_{ij}^E in the above equations are elastic compliance constants at constant electric field. Figure 5 shows the measured and calculated $\epsilon_{33}^T/\epsilon_0$. The relative error $|\epsilon_{33}^T(\text{cal}) - \epsilon_{33}^T(\text{meas})|/\epsilon_{33}^T(\text{meas})$ is below 1.1% for data in the whole temperature range. Furthermore, the piezoelectric stress constant d_{33} calculated from Eq. (14) is compared with that from Eq. (15).

$$d_{33} = \sqrt{(s_{33}^E - s_{33}^D)\epsilon_{33}^T}, \quad (15)$$

where s_{33}^D is the elastic compliance constant at constant electric displacement field. The circles and stars in Fig. 6 are d_{33} calculated from Eqs. (14) and (15), respectively. The relative error of them is below 1.1% for all temperatures. In addition, it is easy to verify that the inversion results obey the condition of thermodynamic stability: $(c_{11}^E + c_{12}^E)c_{33}^E > 2(c_{13}^E)^2$.

The electromechanical coupling coefficient k_{33} is insensitive to temperature variations, and its value calculated from the full tensor data is about 0.88 for all temperatures.

In summary, the temperature dependence of full tensor constants of $[001]_c$ poled Mn-doped 0.24PIN-0.46PMN-0.30PT single crystals has been determined in the temperature range from 25 °C to 55 °C using only one sample. These constants are critically important for the simulation design and performance evaluation of electromechanical devices

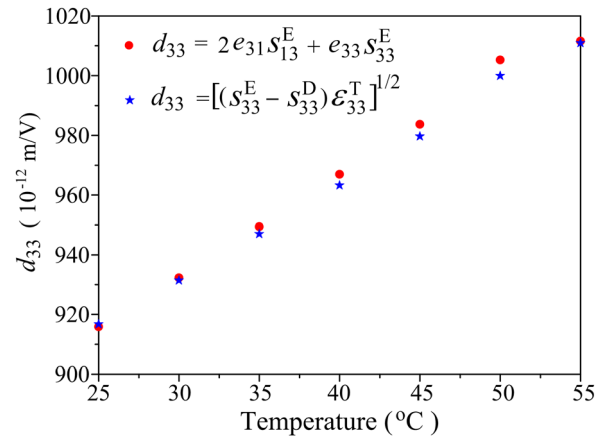


FIG. 6. The temperature dependence of d_{33} calculated using Eqs. (14) and (15) based on the obtained full tensor properties.

based on $[001]_c$ poled Mn-doped 0.24PIN-0.46PMN-0.30PT single crystals.

To ensure the RUS being implemented correctly, the missing modes and overlapped modes must be correctly identified. Because the RUS technique needs to measure a large number of modes, it cannot be used to determine the full tensor material constants of low Q materials ($Q < 100$).¹⁸

This work was supported by the National Natural Science Foundation of China (Grant No. 11374245), the NIH under Grant No. P41-EB2182, and the Natural Science Foundation of Fujian Province, China (Grant No. 2013J01163).

¹P. Sun, Q. F. Zhou, B. P. Zhu, D. W. Wu, C. H. Hu, J. M. Cannata, J. Tian, P. D. Han, G. F. Wang, and K. K. Shung, *IEEE Trans. Ultrason., Ferroelectr., Freq. Control* **56**, 2760 (2009).

²Y. Chen, K. H. Lam, D. Zhou, Q. W. Yue, Y. X. Yu, J. C. Wu, W. B. Qiu, L. Sun, C. Zhang, H. S. Luo, H. L. W. Chan, and J. Y. Dai, *Sensors* **14**, 13730 (2014).

³S. J. Zhang and F. Li, *J. Appl. Phys.* **111**, 031301 (2012).

⁴S. J. Zhang, F. Li, N. P. Sherlock, J. Luo, H. J. Lee, R. Xia, R. J. Meyer, Jr., W. Hackenberger, and T. R. Shrout, *J. Cryst. Growth* **318**, 846 (2011).

⁵E. W. Sun, R. Zhang, F. M. Wu, B. Yang, and W. Cao, *J. Appl. Phys.* **113**, 074108 (2013).

⁶Y. L. Wang, E. W. Sun, W. Song, W. C. Li, R. Zhang, and W. Cao, *J. Alloys Compd.* **601**, 154 (2014).

⁷W. Cao and G. R. Barsch, *Phys. Rev. B* **38**, 7947 (1988).

⁸W. Cao, G. R. Barsch, W. H. Jiang, and M. A. Breazeale, *Phys. Rev. B* **38**, 10244 (1988).

⁹R. G. Sabat, B. K. Mukherjee, W. Ren, and G. Yang, *J. Appl. Phys.* **101**, 064111 (2007).

¹⁰L. G. Tang and W. Cao, *Appl. Phys. Lett.* **106**, 052902 (2015).

¹¹S. J. Zhang, S. M. Lee, D. H. Kim, H. Y. Lee, and T. R. Shrout, *J. Appl. Phys.* **102**, 114103 (2007).

¹²V. Y. Topolov, *Appl. Phys. Lett.* **96**, 196101 (2010).

¹³V. Y. Topolov and C. R. Bowen, *J. Appl. Phys.* **109**, 094107 (2011).

¹⁴I. Ohno, *Phys. Chem. Miner.* **17**, 371 (1990).

¹⁵A. Migliori and J. L. Sarrao, *Resonant Ultrasound Spectroscopy* (Wiley Press, 1997).

¹⁶J. J. Moré, B. S. Garbow, and K. E. Hillstom, User Guide for MINPACK-1, Argonne National Laboratories Report No. ANL-80-74, 1980.

¹⁷J. Pujol, *Geophysics* **72**, W1 (2007).

¹⁸B. J. Zadler, J. H. L. Le Rousseau, J. A. Scales, and M. L. Smith, *Geophys. J. Int.* **156**, 154 (2004).